CHARACTERIZATION OF SILICA-BASED REVERSED-PHASE COLUMNS WITH RESPECT TO RETENTION SELECTIVITY

SOLVOPHOBIC EFFECTS

P. E. ANTLE* and A. P. GOLDBERG

Biomedical Products Department, E. I. du Pont de Nemours and Company, Wilmington, DE 19898 (U.S.A.)

and

L. R. SNYDER

Lloyd R. Snyder, Inc., 2281 William Court, Yorktown Heights, NY 10598 (U.S.A.)

(Received November 7th, 1984)

SUMMARY

Variations in retention and retention selectivity are common among different reversed-phase columns. These retention differences arise from both solvophobic and chemical effects. Solvophobic contributions were studied for seven columns differing in either surface area or composition of the bonded phase. Resulting differences in solute retention were correlated with three effects: (1) the effective phase ratio of the column as measured by the average retention of all solutes; (2) the polarity of the bonded phase; and (3) the dispersion solubility parameter of the bonded phase. These three factors largely determine differences in solvophobic selectivity among different reversed-phase columns.

INTRODUCTION

Packing materials used for reversed-phase high-performance liquid chromatography (RP-LC) differ in the nature of the initial silica particle, the silane used to form the bonded phase, and the bonding process. The resulting column packing can exhibit considerable chemical and physical diversity, as summarized in Table I. These differences in packing characteristics in turn lead to changes in solute retention and band spacing, as has been reported in numerous studies (*e.g.*, refs. 1–21). However, there is as yet little general agreement on the relative importance of the factors summarized in Table I in affecting solute retention. Indeed, column characteristics other than those listed may be of even greater importance in this regard.

Retention in RP-LC systems is the result of both solvophobic interactions[22] and chemical complexation involving solute molecules and reactive species in the stationary phase. Solvophobic retention primarily involves interactions between solute molecules and the organic bonded phase. Chemical complexation effects include hydrogen bonding with unreacted surface silanol groups, ion exchange with these

TABLE I

PROPERTIES OF REVERSED-PHASE COLUMN PACKINGS THAT MAY LEAD TO DIFFER-
ENCES IN RETENTION

Property	Typical range	Ref.
Silica structure		
Pore diameter	6–30 nm	1, 2
Surface area	100–500 m²/g	1–3
pH	4–10	2
Surface contamination by metals	—	4
Bonding silane		
Functionality	C_1, C_8, C_{18}, cyanopropyl, phenyl, etc.	5–11
Mono- *vs.* polychloro	Trialkylchloro *vs.* dialkyldichloro or monoalkyl-trichloro	1, 12, 13
Bonding process		
"Fully bonded" *vs.* partial bonding	1–4.5 μmoles/m²	2, 12–14
With or without endcapping	—	12, 13

same groups, and complexation with trace metals on the silica surface (*e.g.*, refs. 4 and 23–25). In many RP-LC systems both solvophobic and chemical effects are present; therefore these systems will be quite complicated as regards the overall retention process. Chemical selectivity effects can be suppressed to a large extent by using fully-bonded packings made from monofunctional silanes, as well as by choosing mobile phase compositions (additives such as triethyl amine, higher ionic strength, appropriate pH, etc.) that tend to suppress secondary retention for a given sample. Since chemical selectivity is often associated with undesirable separation characteristics, such as band-tailing and column-to-column irreproducibility, we recommend the use of conditions that minimize secondary retention and chemical selectivity. This then leaves solvophobic selectivity as the main effect available when changing columns to vary column selectivity.

Many previous studies have examined different aspects of solvophobic retention (*e.g.*, refs. 1, 5, 6, 9, 11–13, 22 and 26–29). Usually only a narrow range of solutes were studied or no comparisons were made among different column types. Consequently, there are no broad generalizations that can be applied to the classification of different columns with respect to differences in solvophobic retention. In the present study we have attempted to reexamine this question by collecting retention data for several columns differing in surface area or the type of bonded phase, using a number of structurally diverse compounds as solutes. The results of our initial study provide considerable insight into how column selectivity varies with column type; *e.g.*, bonding-phase silane and particle surface area. This should prove useful in identifying column types of unique selectivity for use in retention optimization (band spacing control).

A simplified practice-oriented account of the following analysis has been published[30]. That article can be referred to for further practical insights into column selectivity in reversed-phase separation.

THEORY

Model for solvophobic retention effects in reversed-phase HPLC based on gradient elution data

As will be described in the Experimental section, the retention of various solutes on different columns was studied in the gradient elution mode. Most previous studies of reversed-phase retention have employed isocratic elution rather than gradient elution. However, there are several reasons for preferring gradient elution as used here. This is illustrated in the plots of Fig. 1, where retention is shown as a function of organic content of the mobile phase for three hypothetical compounds, A, B and C. The quantity k' refers to the isocratic retention factor and φ is the volume fraction of the organic portion of the mobile phase. Such plots are linear to a first approximation (*cf.*, refs. 22, 31). Retention data are collected most accurately and conveniently within a relatively narrow range of k' values, typically $1 \leqslant k' \leqslant 10$. Furthermore, most isocratic HPLC assays restrict k' values within a similar narrow range; therefore, for practical applicability, we desire values of k' within this range for all compounds studied.

In Fig. 1 we see that it is not possible to obtain good retention data for compounds A–C in a single isocratic run (a single value of φ); the k' range for the illustrated solutes is simply too great. However, in linear-solvent-strength (LSS) gradient elution[31] every solute elutes with the same average k' value, $\bar{k}$, where

$$\bar{k} = t_G/(1.15\, t_0\, S\, \Delta\varphi) \tag{1}$$

Here t_G is the time during which the mobile phase composition changes (gradient time), t_0 is the column dead time, and $\Delta\varphi$ is the range of the gradient [φ (final) $- \varphi$ (initial)]. S is a measure of the dependence of $\log k'$ on mobile phase composition, φ, for a given solute, and is equal to $-d(\log k')/d\varphi$; *i.e.*, $-S$ equals the slopes of plots as in Fig. 1. Since values of S for small solute molecules (200–1000 daltons) are roughly constant (equal to 5–10), eqn. 1 demonstrates that LSS gradient elution solves the major problem indicated in Fig. 1. That is, a single gradient run can yield retention data for a wide range of solutes, all within the optimum k' range. Further
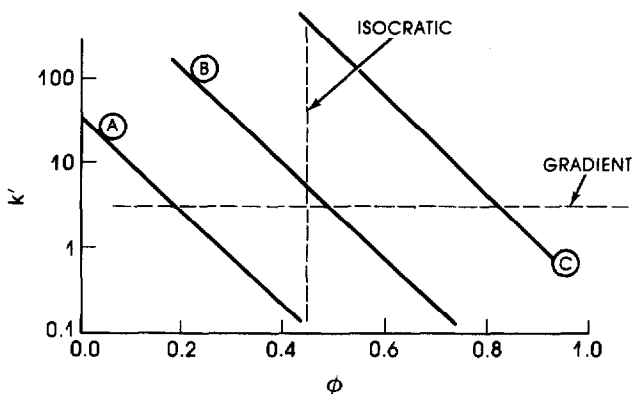

Fig. 1. Hypothetical plots of retention (k') *vs.* mobile phase composition (φ) for three solutes A, B and C. Isocratic *vs.* gradient separation.

advantages of using gradient rather than isocratic data collection include: (a) multiple solutes (both weakly and strongly retained compounds) can be run simultaneously within a given standardized run in minimum time, (b) the use of a single set of chromatographic conditions for all solutes facilitates automated data collection and the use of unattended runs, and (c) experimental conditions do not have to be varied for different columns and/or solutes.

For linear-solvent-strength (LSS) systems as used here there exists a comprehensive and detailed theory (*e.g.*, refs. 31–33) which relates gradient and isocratic retention values. The retention time, t_g, for a solute in LSS gradient elution is given by

$$t_g = (t_0/b) \log (2.3 \, k_0 b + 1) + t_0 + t_D \tag{2}$$

where t_D is the gradient-unit dwell time (time spent by mobile phase between the gradient mixer and the column inlet), k_0 is the isocratic k' value for the solute in the initial mobile phase of the gradient, and b is a gradient steepness parameter defined as

$$b = t_0 \, S \, \Delta\varphi/t_G = 1/(1.15\bar{k}) \tag{3}$$

For most solutes we can simplify eqn. 2 to

$$t_g \approx (t_0/b) \log (2.3 \, k_0 b) + t_0 + t_D \tag{4}$$

In reversed-phase HPLC we can relate a value of k' or k_0 to the phase ratio of the system, ψ_i:

$$k_{xi} = K^0_{xi} \, \psi_i \tag{5}$$

The quantity k'_{xi} refers to the k_0 value for compound X and reversed-phase column i under a given set of isocratic conditions (φ specified) and K^0_{xi} is a distribution constant for solute X, column i, and a given value of φ.

There is presently some question over how the phase ratio is defined for reversed-phase systems. it can be argued that ψ is proportional either to the bonded phase surface area or to its total volume (adsorption *vs.* partition processes). In fact, ψ is probably determined by both the surface area and the volume of the bonded phase. Literature data (*e.g.*, ref. 34) suggest that there is little increase in retention on a C_8 column *vs.* a C_{18} column, whereas the volume of stationary phase is roughly double on the C_{18} column. This suggests that surface-area effects are more important. However, the effective surface area of the bonded phase decreases while alkyl chain length is increasing (*e.g.*, ref. 35); so the net result of increasing chain length from C_8 to C_{18} probably involves compensating effects (see also the discussion of ref. 22, pp. 151–159).

The value of K^0_{xi} will depend on the polarity P_i of the column i, and to a first approximation we can write

$$k_{xi} = K_{xi} \, f(P_i) \, \psi_i \tag{6}$$

Eqn. 6 recognizes (as we will see in a following section) that reversed-phase retention generally decreases for all compounds as stationary phase polarity increases (and approaches that of the mobile phase). The polarity of bonded phases appears to increase when polar groups (*e.g.*, cyano) are introduced or when the alkyl chain length is decreased (probably due to lesser shielding of surface silanol groups on the silica matrix). It will prove convenient to combine the phase-ratio and stationary-phase polarity effects into a single parameter J':

$$J' = \log \psi_i + \log [f(P_i)] \tag{7}$$

So that

$$\log k_{xi} = \log K_{xi} + J'_i \tag{8}$$

The primary effect of the phase ratio/polarity term J'_i on retention of a solute X is to change the gradient-retention of X by a fixed amount. We can therefore regard J' as the effective phase ratio for column i, or as a measure of the strength of a column (stronger columns mean larger values of J'). We can correct for this effect (change in J'_i) by comparing values of t_g from column i $[(t_g)_{xi}]$ with values for a reference column r (Zorbax C-8®*, 330 m²/g, in this study); *i.e.*, by taking the difference in t_g values for the two columns and solute X:

$$(\Delta t_g)_{xi} = (t_g)_{xi} - (t_g)_{xr} \tag{9}$$

It is assumed that gradient conditions are maintained the same (only the column is changed), which means that $\Delta\varphi$, t_0 and t_G remain constant. Combination of eqns. 3, 4 and 8 ($k_{xi} \approx k_0$) with eqn. 9 then leads to

$$(\Delta t_g)_{xi} = [t_G/(\Delta\varphi S_x)] [\log (K_{xi}/K_{xr}) + J'_i - J'_r] \tag{10}$$

Here K_{xr} and J'_r refer to values of K_{xi} and J'_i for the reference column r. Eqn. 10 assumes that values of S for solute X are the same on column i and column r. This appears to be a reasonable approximation; one study[36] has shown that S values on a cyanopropyl column are equal to 1.1 times the corresponding S values (solutes) for a C_{18} column. Since these two reversed-phase column types will be shown to represent extremes, actual differences in S values among other columns should be less than 10% for a given solute. That is, S can be regarded as a function of the solute, J' is a function of the column, and (K_{xi}/K_{xr}) is a function of both solute and column.

Eqn. 10 predicts that a significant contribution to column selectivity will arise from the combination of (a) columns of different J' values and (b) solutes A and B having different S values (S_a, S_b). There will also be a further contribution to band-spacing and column selectivity from the solute–column interaction term (K_{xi}/K_{xr}). K_{xi} and K_{xr} refer approximately to the thermodynamic distribution constants for solute X and columns i and r, respectively; *i.e.*, K_{xi} reflects specific interactions of solute X and bonded-phase i**.

---

* Zorbax is a registered trademark of DuPont for its LC columns and packings.

** In terms of the actual distribution constants K^0_{xi} and K^0_{xr}, we see (eqns. 5 and 6) that (K_{xi}/K_{xr}) = $(K^0_{xi}/K^0_{xr}) [f(P_r)/f(P_i)]$ = (constant) (K^0_{xi}/K^0_{xr}) for a given pair of columns i and r and various solutes X.

We will define the relative phase-ratio/polarity term J_i as

$$J_i = J_i' - J_r'$$ (11)

that is, J_i is the phase-ratio/polarity parameter for column i relative to reference column, r. Eqn. 10 can now be written as

$$(\Delta t_g)_{xi} = [t_G/(\Delta\varphi S_x)] \, [\log (K_{xi}/K_{xr}) + J_i]$$ (12)

A standard column (s) for which (K_{xi}/K_{xr}) is approximately equal to unity is next selected; namely, a lower surface-area (larger-pore) column with the same bonded phase as the reference column r. This simplifies eqn. 12 for the standard column to

$$(\Delta t_g)_{xs} = t_G \, J_s/(\Delta\varphi S_x)$$ (13)

Here we use a 330 m^2/g Zorbax C-8 packing for the reference column (r) and a 140 m^2/g Zorbax C-8 as the standard column (s). Ignoring solute–column interactions (the K_{xi}/K_{xr} term) apart from average interactions that determine the average values of J_i, eqn. 12 then becomes

$$\overline{(\Delta t_g)_{xi}} = [t_G/(\Delta\varphi \overline{S})] \, [\overline{\log (K_{xi}/K_{xr})}] + [t_G/\Delta\varphi S_x)] \, (J_i)$$ (14)

Here $\overline{(\Delta t_g)_{xi}}$ and $\overline{\log (K_{xi}/K_{xr})}$ represent the average values of $(\Delta t_g)_{xi}$ and $\log (K_{xi}/K_{xr})$, and $\overline{S}$ is the average value of S_x for the entire solute set.

From eqn. 13,

$$t_G/(\Delta\varphi S_x) = (\Delta t_g)_{xs}/J_s$$ (15)

and substituting eqn. 15 into eqn. 12 gives

$$(\Delta t_g)_{xi} = (J_i/J_s) \, (\Delta t_g)_{xs} + [t_G/(\Delta\varphi S_x)] \, \overline{\log (K_{xi}/K_{xr})}$$ (16)

or

$$(\Delta t_g)_{xi} = m \, (\Delta t_g)_{xs} + a$$ (17)

If values of (K_{xi}/K_{xr}) for each solute were constant, then values of m and a would also be constant, with

$$m_i = J_i/J_s$$ (18)

Since values of (K_{xi}/K_{xr}) will generally vary with the column and solute, reflecting specific column–solute interactions, eqn. 16 is not exact, and we can write

$$(\Delta t_g)_{xi} = m_i \, (\Delta t_g)_{xs} + a + \Delta(\Delta t_g)_{xi}$$ (19)

Values of $\Delta(\Delta t_g)_{xi}$ are seen to equal the deviations of experimental $(\Delta t_g)_{xi}$ values from best-fit plots to eqn. 17. Now substitution of m_i from eqn. 18 into eqn. 19 yields

$$\Delta(\Delta t_g)_{xi} = (\Delta t_g)_{xi} - (J_i/J_s)(\Delta t_g)_{xs} - a \tag{20}$$

Finally, $(\Delta t_g)_{xi}$ from eqn. 12 and $(\Delta t_g)_{xs}$ from eqn. 13 can be substituted into eqn. 20 to obtain

$$\Delta(\Delta t_g)_{xi} = [t_G/(\Delta \varphi S_x)] \log (K_{ir}/K_{xr}) - a$$
$$\approx [t_G/(\Delta \varphi \bar{S})] \log (K_{ir}/K_{xr}) - a \tag{21}$$

The quantity $\Delta(\Delta t_g)_{xi}$ is seen to be linearly related to the quantity $\log (K_{xi}/K_{xr})$, which is in turn proportional to the differences in free energies of retention of X on column i vs. column r*. The quantity $\Delta(\Delta t_g)_{xi}$ can therefore be manipulated in the same fashion as is used to correlate values of $\log k_i = R_M$ with solute molecular structure. That is, we can use values of $\Delta(\Delta t_g)_{xi}$ to analyze the origin of the second-order column-selectivity effects arising from the (K_{xi}/K_{xr}) term.

In reversed-phase systems we expect adherence of solute retention data to the Martin equation[37]:

$$R_M = \Sigma (\Delta R_M) \tag{22}$$

where the value of R_M for a given solute and HPLC system is the sum of contributions ΔR_M from each group i in the solute molecule. For the case of homologous series, the corresponding equation for values of $\Delta(\Delta t_g)_{xi}$ is

$$\Delta(\Delta t_g)_{xi} = C_1 n + C_3 \tag{23}$$

where n is the number of repeating structural units (e.g., methylenes) and C_3 is a constant for a given parent solute molecule ($n = 0$) and specified HPLC system. Here the constant C_1 will be larger for stronger interaction of the repeating unit with a particular column.

For the case of two types of repeating units in the solute molecule, aliphatic (n) and aromatic (m) carbon atoms, we can write

$$\Delta(\Delta t_g)_{xi} = C_1 n + C_2 m + C_3 \tag{24}$$

Likewise, linear free energy relationships can be anticipated of the form

$$\Delta(\Delta t_g)_{xi} = C_4 \Delta(\Delta t_g)_{xj} + C_5 \tag{25}$$

where j refers to a second column (other than i).

Eqn. 25 would be applicable whenever a single physical effect (e.g., "polar"

---

* K_{xi} and K_{xr} are related to k_0 of eqn. 2; therefore, values of K refer to the starting mobile phase in the gradient. However, since S_x is assumed constant for columns i and r, (K_{xi}/K_{xr}) will be constant for any value of φ.

interaction) primarily determines the values of (Δt_g) on the two columns. The applicability of eqns. 24 and 25 to reversed-phase systems will be shown in a following section.

Change in gradient time

Let us next examine the effect on t_g of a change in the gradient time, t_G, using the same column. Assume runs 1 and 2, with gradient times t_{G1} and t_{G2} where $t_{G2} = 2 t_{G1}$. The retention times for a solute are t_{g1} and t_{g2}. Combination of eqns. 3 and 4 then allows us to write

$$t_{g1} = [t_{G1}/\Delta\varphi S_x)] (\log 2.3 \ k_0 t_0 \Delta\varphi S_x - \log t_{G1}) + t_0 + t_D \tag{26}$$

and

$$t_{g2} = [2t_{G1}/(\Delta\varphi S_x)] [\log 2.3 \ k_0 t_0 \Delta\varphi S_x - \log (2 \ t_{G1})] + t_0 + t_D \tag{27}$$

Combination of eqns. 26 and 27 then yields

$$t_{g1} - (t_{g2}/2) = [t_{G1}/(\Delta\varphi S_x)] \log 2 + (t_0 + t_D)/2 \tag{28}$$

Finally, for two separate runs on the reference column, eqn. 15 and 28 combine to give

$$t_{g1} - (t_{g2}/2) = [(\Delta t_g)_{xs}/J_s] [\log 2] + (t_0 + t_D)/2 = w(\Delta t_g)_{xs} + r \tag{29}$$

Eqn. 29 predicts that plots of $[t_{g1} - (t_{g2}/2)]$ *vs.* $(\Delta t_g)_{xs}$ will be linear (i.e. w and r are constant). Inasmuch as the (K_{xi}/K_{xr}) term does not enter into the derivation of eqn. 29, eqn. 29 should also be more precise and independent of specific column–solute interactions, *vs.* eqn. 17. Thus comparing the results predicted by eqn. 29 with experimental data offers a further check on the validity of the present model.

Eqn. 29 also provides another piece of information: the slope of a plot of $[t_{g1} - (t_{g2}/2)]$ for two runs on the reference column *vs.* $(\Delta t_g)_{x,s}$ yields a value of J_s which cannot otherwise be obtained.

EXPERIMENTAL

Chromatographic data were obtained using a Du Pont four-solvent gradient LC system (E. I. du Pont de Nemours and Company, Wilmington, DE, U.S.A.), which utilizes a three-head reciprocating piston pump. Gradient formation is accomplished with a built-in low-pressure mixing chamber and magnetic stirring. A filter containing a 2-μm element is included at the outlet of the pump. A Valco six-port injection valve (Valco Instrument Company, Houston, TX, U.S.A.) is used in conjunction with a Du Pont 834 autosampler for automated operation. The injection valve and column were enclosed in a Du Pont column compartment (air bath) at 50°C. The detector was a Du Pont 851 filter photometric detector using a low-pressure mercury lamp to provide absorbance measurements at 254 nm. Retention times were obtained from a Spectra-Physics 4100 integrator (Spectra-Physics, Santa Clara, CA, U.S.A.).

TABLE II

COLUMN SPECIFICATIONS

Column	Surface modification	Endcapping	Surface area (m^2/g)	Median pore diameter (nm)	% C	Coverage $(\mu mole/m^2)$
Zorbax ODS	CH₃ | – Si–n(C₁₈H₃₇) | CH₃	None	330	7	16	2.6
Zorbax C-8 (reference)	CH₃ | – Si–n(C₈H₁₇) | CH₃	(CH₃)₃–Si–	330	10	10	3.0
Zorbax 150-C8 (standard)	CH₃ | – Si–n (C₈H₁₇) | CH₃	(CH₃)₃–Si–	140	17	6	3.2
Zorbax Phenyl	CH₃ | – Si–(CH₂)₂–(C₆H₅) | CH₃	(CH₃)₃–Si–	300	9	8	3.0
Zorbax CN	CH₃ | – Si–(CH₂)₃–CN | CH₃	None	310	9	6	3.5
Zorbax TMS	–Si–(CH₃)₃	Undisclosed	320	8	4	3.7
Chromegabond FD	[CH₃ | – Si–(CH₂)₂–n(C₈F₁₇) | CH₃]*	(CH₃)₃–Si–	500	6	8 (19% F)	NA

* Ref. 39.

Data manipulation was performed with an HP-87 personal computer (Hewlett-Packard, Corvallis, OR, U.S.A.) using Visicalc® PLUS spreadsheet, and plotting software.

The columns used in this study are listed in Table II along with data on their physical and chemical characteristics. All data were provided by the manufacturers except the identity of the derivatizing reagent in the FD column[39]. Commercial 25 × 0.46 cm Zorbax columns were obtained from Du Pont. The 30 × 0.46 cm Chro-

TABLE III

SOLUTES USED IN PRESENT STUDY

Name	Supplier*	$(\Delta t_g)_{xs}$		No. of C		No. of polar groups
		Acetonitrile	Methanol	Ali-phatic	Aro-matic	
Benzyl alcohol	A	−1.09	−0.87	1	6	1
Butyl paraben	S	−0.91	−0.47	5	6	2
Chlorpropham, CIPC	P	−1.01	−0.62	4	6	2
Corticosterone	R	−0.74	−0.44	21	0	4
Cortisone	R	−0.60	−0.42	21	0	5
Dexamethasone	R	−0.58	−0.37	22	0	5
Dioctylphthalate	A	−	−	18	6	2
Dibutylphthalate	C	−1.06	−0.52	10	6	2
Diethylphthalate	C	−1.02	−0.61	6	6	2
Dimethylphthalate	A	−	−	4	6	2
Ethyl paraben	S	−	−0.53	3	6	2
Fluorobenzene	A	−1.28	−1.16	0	6	0
Hexafluorobenzene	A	−1.14	−0.97	0	6	0
Methyl paraben	S	−0.92	−0.54	2	6	2
Methyl benzyl amine	A·	−1.14	−	2	6	1
1-Methylnaphthalene	A	−	−	1	10	0
1-Methylphenan-threne	A	−	−	1	14	0
o-Nitrophenol	C	−1.01	−	0	6	2
Propachlor, Ramrod	P	−0.97	−0.64	5	6	2
Propyl paraben	S	−	−0.50	4	6	2
Toluene	K	−	−	1	6	0
Tri-p-tolyl phosphate	K	−0.99	−0.41	3	18	1

    * A = Aldrich, Milwaukee, WI, U.S.A.; C = Chem Service, West Chester, PA, U.S.A.; K =
Eastman-Kodak, Rochester, NY, U.S.A.; P = PolyScience Corp., Niles, IL, U.S.A.; R = Roussel Corp.,
New York, NY, U.S.A.; S = Sigma, St. Louis, MO, U.S.A.

megabond column was from ES Industries (Vineland, NJ, U.S.A.).

    The solvents for this study were Baker Analyzed reagent grade (J. T. Baker
Chemical Company, Phillipsburg, NJ, U.S.A.). The compounds used as test solutes
are listed in Table III and were obtained from a variety of sources, as indicated by
the single letter after the compound name.

    The solutes were initially run individually. Based on these data, compounds
were chosen which were expected to be well spaced in the gradient, and mixed samples
were made. These contained up to five solutes. Identification of the peaks was ac-
complished by peak area and elution order. If elution order changes were noted in
any run, new mixtures were made to confirm peak assignments. Each column was
run for at least two data sets on separate days. Each data set consisted of at least
duplicate measurements for each solute. One "standard" compound* was included
in all samples of a data set, to check the reproducibility of the pump and the gradient
generation. In addition, a pressure trace was monitored.

    Standard chromatographic conditions were used for data acquisition. A linear

_____

    * Either benzyl alcohol or tri-p-tolyl phosphate.

gradient was run from 5% organic solvent in water to 100% organic solvent over 15 min. Samples were injected in 20-μl volumes at concentration of less than 1 mg/ml. The flow-rate for the 25-cm-long columns was set to 2.5 ml per min. For the 30-cm Chromega column, flow-rate was increased to 3.0 ml/min to provide equivalent values of b, as for the other (25-cm) columns. Since the dwell volume of the system is approximately 6 ml, the higher flow-rate for the Chromega column yields a lower t_D value, requiring subtraction of 0.4 min (6/2.5 − 6/3.0) from experimental values of t_g for this column, to yield values comparable to those for the other columns.

RESULTS AND DISCUSSION

In the present study we attempted to avoid selecting our test solutes on too narrow a basis. We therefore initially chose a group of solutes which included both simple molecules of varying functionality plus a random assortment of more complex molecules from "real world" compounds. These solutes were then run in our standard gradient system, which has no buffers or additives (*e.g.*, amines) in the mobile phase. Any compound with detection or peak shape problems was excluded at this point. In this way, it was felt that we had largely eliminated solutes which might exhibit complexation effects, and restricted data collection to compounds which could conveniently provide reproducible retention data. After initial selectivity data were obtained in acetonitrile–water gradients with this group of 15 solutes, similar experiments were performed with methanol–water gradient for 13 of the original 15 solutes plus ethyl and propyl paraben. Additional experiments were later carried out using other solutes, in order to explore the specific contributions of alkyl and aromatic carbons to solute retention. A total of 22 solutes were used in all, as summarized in Table III. Also listed in Table III are the $(\Delta t_g)_{xs}$ values for each compound in acetonitrile and methanol, plus the number of aliphatic and aromatic carbons and "polar" substituent groups (subjectively assigned).

All columns but one from Table II are based on Zorbax-SIL as substrate for the bonded phase. The pore geometry of Zorbax particles is quite reproducible and regular (densely packed microspheres) and therefore should not introduce additional selectivity effects among the columns. These columns include the major types presently in use: long, medium and short alkyl chains (ODS, C-8, and TMS), aromatic (Phenyl), and cyano (CN). More limited data were also collected for a fluorodecyl (FD) column, in view of the special selectivity effects which have been reported for this phase[10,11,38,39].

Comparison of retention data with the present model
The averaged retention data in acetonitrile for the 22 test solutes using the various columns are included in Appendix I. It was observed that within-day repeatability of these data was about ±0.015 min, while day-to-day repeatability averaged ±0.06–0.16 (1 S.D.). A ±0.02 min (1 S.D.) variation was found previously for the gradient retention of dialkyl phthalates in a similar gradient system[33]. The greater variability of the present data may reflect the more diverse solute structures represented by the present test compounds. The actual error in reported values of t_g should be less than 0.06–0.16 min, because a minimum of two runs on different days were made for each column–solute combination, with final results averaged.

TABLE IV

SUMMARY AND CORRELATION OF RETENTION DATA (ACETONITRILE–WATER)

Column	$(\overline{\Delta t_g})_{xi}$ (min)	$\Delta\varphi$ vs. ODS (%)	Correlations from Fig. 3			Standard deviations*
			m	a	r	
ODS	0.10	0	−0.80	−0.67	0.55	0.28 (0.24/0.15)
C-8 330 m²/g (reference)	(0.00)	− 1	(0.00)	(0.00)	−	−
C-8 140 m²/g (standard)	−0.67	− 5	(1.00)	(10.00)	−	−
Phenyl	−0.96	− 7	1.69	0.96	0.81	0.41 (0.24/0.33)
TMS	−1.88	−13	3.39	1.39	0.94	0.70 (0.25/0.66)
CN	−2.83	−19	5.14	2.13	0.95	1.05 (0.34/1.00)
FD	−2.96	−20	0.70	−2.28	0.22	0.62 (0.60/0.14)
C₈ 330 m²/g; $t_G = 30$	−	−	0.93	−2.07	0.92	0.19 (0.08/0.18)

* $X(Y/Z)$ format refers to: X = the total standard deviation for Δt_g values due to phase ratio/ polarity and column–solute interactions; Y = the standard deviation around the best-fit lines of Fig. 3 and 6 due to column–solute interactions, and Z = the standard deviation due to phase ratio/polarity.

Following the analysis presented in the Theory section and illustrated in Appendix II, the C_8 column (330 m²/g) was selected as reference column and values of $(\Delta t_g)_{xi}$ for all solutes X and columns i were obtained by subtracting the value of $(t_g)_{xr}$ for the reference column and compound X from corresponding t_g values for X on other columns. The average of $(\Delta t_g)_{xi}$ values for all solutes X and a given column i is defined as $(\overline{\Delta t_g})_{xi}$ and is given in Table IV. These $(\overline{\Delta t_g})_{xi}$ values show that on average a solute elutes at the same k' value from a cyanopropyl column at a mobile phase composition containing 20% less acetonitrile than is required on an ODS column.
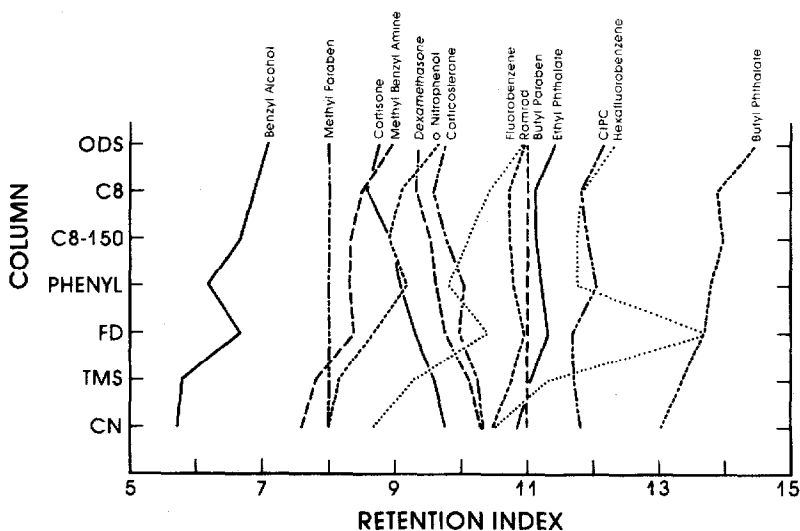

Fig. 2. Relative retention (retention index basis) for present solutes (Table II) on different columns (Table III). Retention index based on methyl paraben equal 8 and butyl paraben equal 11.
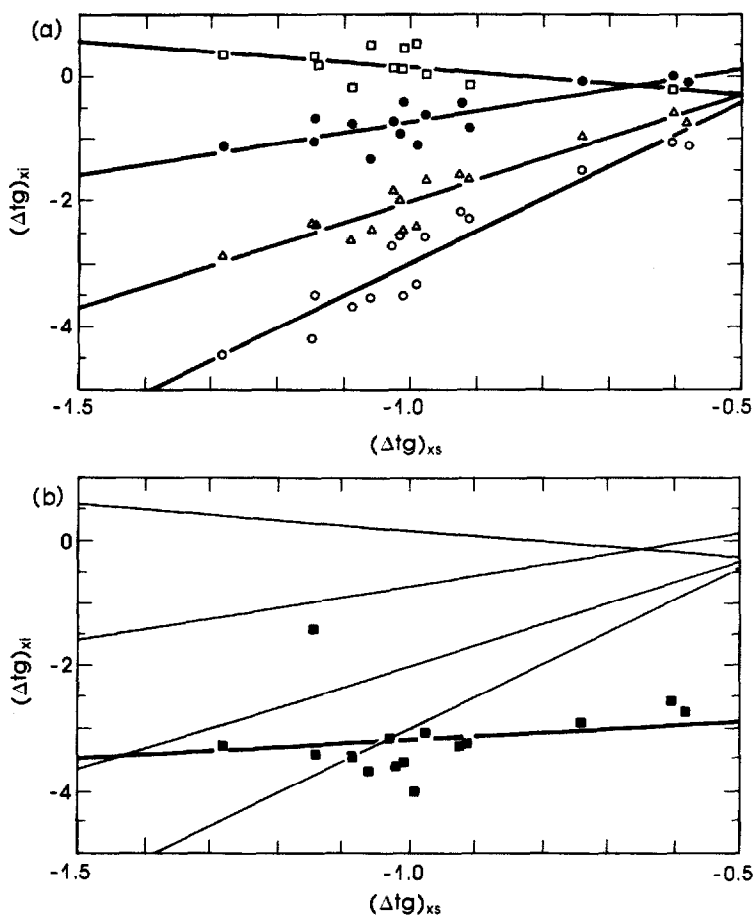
Fig. 3. Correlation of change in solute retention $(\Delta t_g)_{xi}$ for column i vs. $(\Delta t_g)_{xr}$ for column r (Zorbax C-8) according to eqn. 17. Acetonitrile–water mobile phase. (a) Zorbax columns: □, ODS; ●, Phenyl; △, TMS; ○, CN. (b) ■, FD column.

The retentivity of the columns of Table III is: ODS (most retentive) > C-8 (330 m²/g) > C-8 (140 m²/g) > Phenyl > TMS > CN (least retentive).

Differences in retention selectivity or band-spacing on the various columns of Table II are conveniently compared as plots of retention index vs. column type, as shown in Fig. 2 (using methyl and butyl paraben as normalizing compounds). It is apparent from these plots that considerable change in band position occurs from column to column; i.e., significant column selectivity effects exist among this group of columns. Selectivity changes are also seen between the C-8 (330 m²/g) and the lower surface area C-8 (140 m²/g), for which we assume K_{xi}/K_{xr} equal to unity (see also t_g values of Appendix I).

We next evaluated eqn. 17 as a basis for interpreting the selectivity effects for these seven columns. Resulting plots of $(\Delta t_g)_{xi}$ vs. $(\Delta t_g)_{xs}$ are shown in Fig. 3. Data for all columns but fluorodecyl are plotted in Fig. 3a. While some scatter of points exists around the best-fit lines, it is apparent that the $(\Delta t_g)_{xi}$ values for each column correlate reasonable well with corresponding $(\Delta t_g)_{xs}$ values (Table III) for each solute

on the standard (140 m^2/g C-8) column (see correlation data of Table IV). The corresponding plot for the FD column is shown in Fig. 3b, and greater scatter of data points from the best-fit line is evident (see Table VII and related discussion).

The origin of these column-dependent shifts in selectivity is illustrated by the hypothetical plots of Fig. 4a for two solutes X and Y whose S values vary, and for columns i and j with the same type of bonded phase (C_8 in this case) but differing in their surface areas and phase ratios ψ. Linear plots of log k' *vs.* φ are assumed in each case, and it is seen that the retention curves for solute X (or Y) on the two columns are vertically displaced by a fixed amount (eqn. 5 with K^0_{Xi} assumed constant for each column). For isocratic separation of X and Y on each column with the same mobile phase composition φ_1, there is no selectivity difference between columns i and j; *i.e.*, the separation factor α for X and Y equals a constant value for each column. However columns i and j would normally not be used in this fashion (same value of φ for each column and a given sample). Rather, φ will be adjusted to maintain k' values for X and Y in an optimum range (*e.g.*, $k' \approx 2$), as illustrated in Fig. 4b. Here φ-values are selected equal to φ_2 for column i and φ_3 for column j. Now it is seen that the α-values for the two bands (X and Y) are quite different for the two columns. On column i, α is equal to one (same k' value for each compound and no separation), while on column j compound Y has a much smaller k' value than does compound X ($\alpha \approx 4$). Thus the two columns would appear to have quite different selectivity.

A similar result is obtained in gradient elution, when experimental conditions are adjusted to give an average k' value ($\bar{k}$) equal to 2. This is illustrated in Fig. 4c. Here for $\bar{k}_1 \approx 2$, it is seen that compounds X and Y are unseparated on column i, but Y comes out much earlier than X on column j (run with the same gradient conditions, as in our standard gradient). If gradient conditions (*e.g.* t_G) are changed so as to change $\bar{k}$ (eqn. 1) to a value $\bar{k}_2 \approx 4$ (see Fig. 4c), then the separation of X
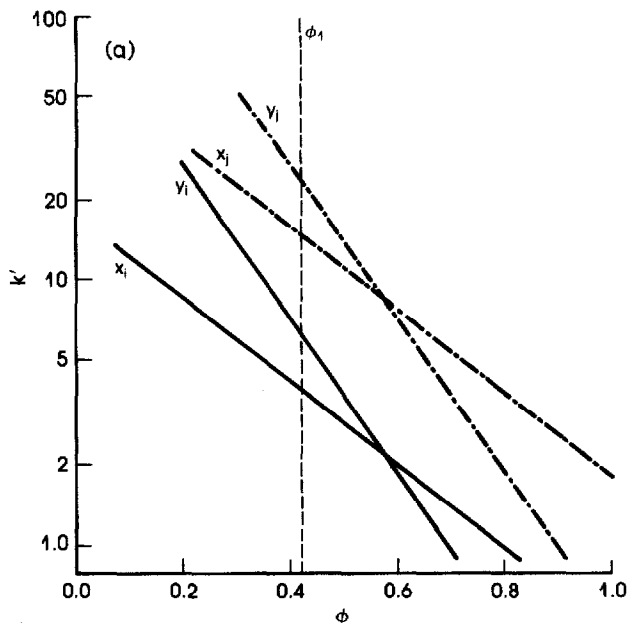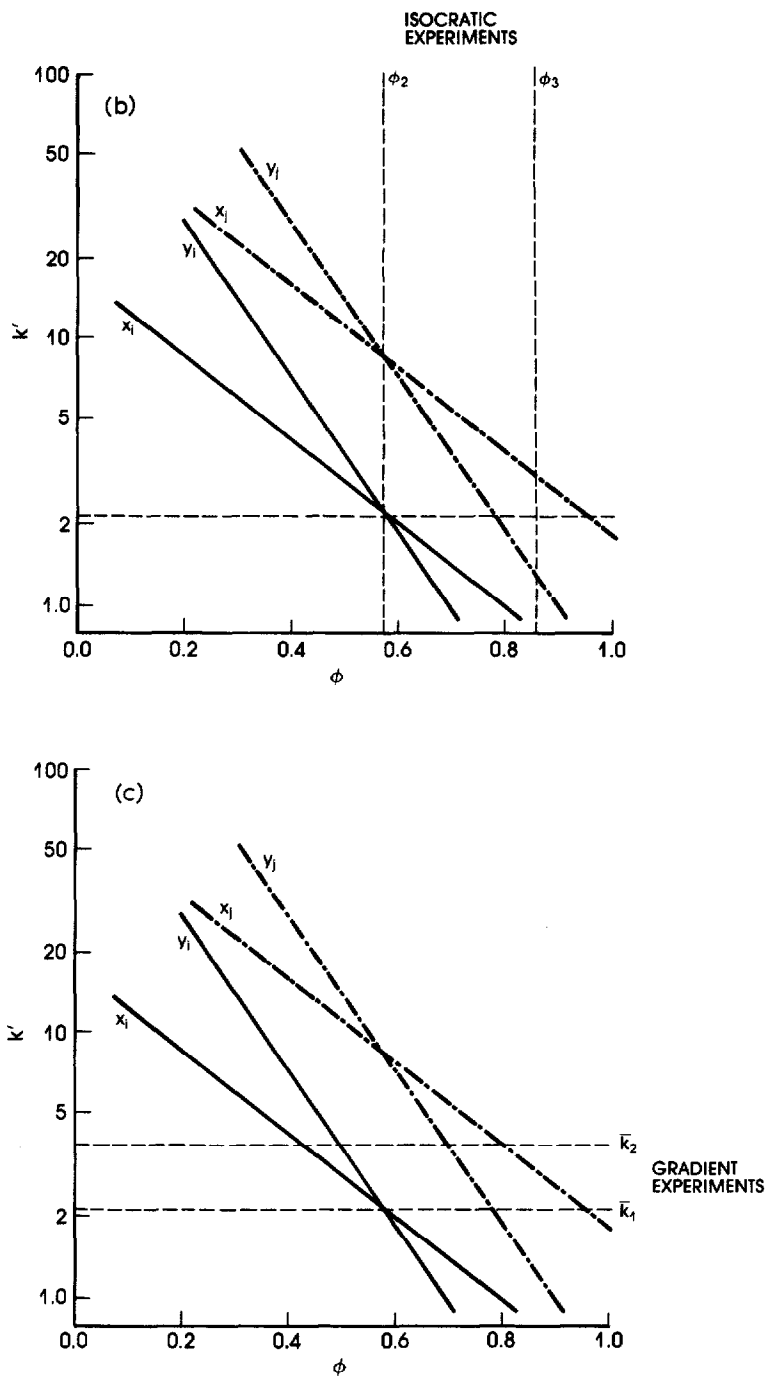

Fig. 4.

Fig. 4. Retention relationships for two solutes X and Y on columns i and j differing only in phase ratio (*e.g.*, two C_8 columns). ———, column i; - · - · -, column j. (a) Separation with mobile phase of $\varphi = \varphi_1$; (b) separation with mobile phase giving values of $k' \approx 2$; (c) gradient separation with $\bar{k} \approx 2$.

and Y on each column is seen to change in a fashion similar to that which results from a change in mobile phase composition φ; see discussion of eqn. 29 and note similarity of eqns. 17 and 29.

The slopes m of plots as in Fig. 3 should be related to the average value $\overline{(\varDelta t_g)}_{xi}$ for each column i:

$$\overline{(\varDelta t_g)}_{xi} = [t_G \, J_s/(\varDelta\varphi\bar{S})] \, m_i + [t_G/(\varDelta\varphi\bar{S})] \log (K_{xi}/K_{xr}) \tag{30}$$

or

$$m_i = [\varDelta\varphi\bar{S}/(t_G \, J_s)] \, \overline{(\varDelta t_g)}_{xi} - (1/J_s) \log (K_{xi}/K_{xr}) = p \, \overline{(\varDelta t_g)}_{xi} + q \tag{31}$$

Here p and q are constants, which assumes values of (K_{xi}/K_{xr}) are small compared to the variation of t_g values as a result of change in J_i and S_x. Eqn. 31 is tested in Fig. 5, and a good correlation is observed for the various columns, with the exception of the fluorodecyl column.

Consider next the application of eqn. 29 to the plot of Fig. 6, where retention data for the reference column and two different gradient times ($t_G = 15$ and 30 min) are plotted vs. values of $(\varDelta t_g)_{xs}$. Larger t_G values result in an increase in the average k' value of each solute during elution (eqn. 1) which is equivalent to a change in φ for isocratic separation. Consequently, a change in t_G results in changes in band-spacing that parallel changes in φ as illustrated in Fig. 4 for different columns, and shown in Fig. 3 for actual data. Thus the plot of Fig. 6 is formally equivalent to similar plots in Fig. 3. The fit of data to the best straight line (eqn. 29) is expected to be much better in Fig. 6 vs. Fig. 3, and this is seen to be the case (Table IV, last column; ± 0.08 S.D. for plot of Fig. 6, vs. ± 0.24–0.60 S.D. for plots of Fig. 3). Thus, for columns of the same bonded-phase type (C_8 in Fig. 6), we expect $(K_{xi}/K_{xr}) = 1$, whereas in Fig. 3 the observed deviations are largely due to non-zero values of log (K_{xi}/K_{xr}) which result from the comparison of columns of different bonded-phase type. From eqn. 29, the slope of the plot in Fig. 6 ($+0.93$) should equal $-(\log 2)/J_s$,
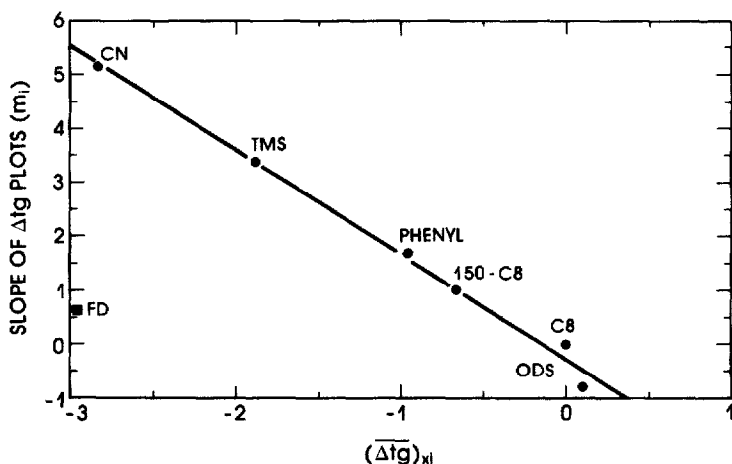

Fig. 5. Correlation of selectivity-slopes m_i from Fig. 3 with column strength $(\varDelta t_g)_{xi}$, according to eqn. 31. Excluding point for FD column, $m_i = -1.94 \, (\varDelta t_g)_{xi} - 0.28 \, (r = 0.996)$.
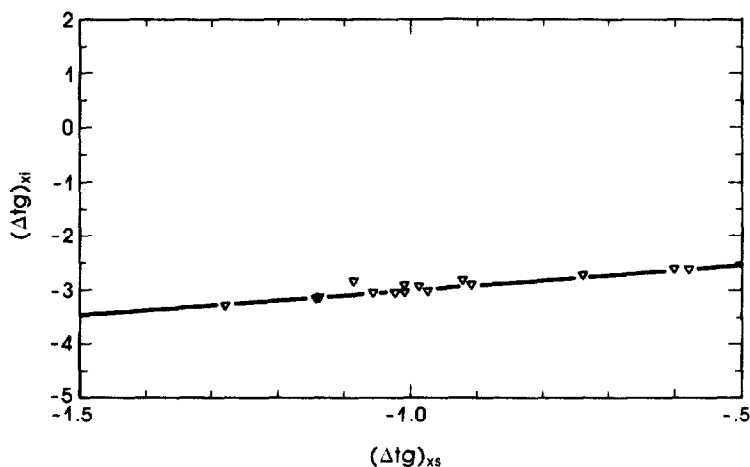
Fig. 6. Change in gradient time t_G mimics changes in column strength (eqn. 29). y-axis equals $[(t_{g2}/2) - t_{g1}]$, where "1" refers to 15-min gradient and "2" refers to 30-min gradient. See Table IV.

which gives $J_s = -0.32$. Eqn. 18 then permits calculation of J_i values for the remaining columns of Table V.

Other contributions to column selectivity

The major column-selectivity effect (that due to the combination of S_x and J_{ir}, Fig. 5) has now been accounted for. This allows us to study remaining selectivity effects due to specific solute–column interactions (values of K_{xi}/K_{xr}) via eqn. 21–25. Retention data for a series of homologues and benzologues were next examined, to analyze the non-J effects in terms of $\Delta(\Delta t_g)_{xi}$, since the J effect is removed from these $\Delta(\Delta t_g)_{xi}$ values which are linearly related to free energies of retention (eqn. 21). Resulting $\Delta(\Delta t_g)$ values were found to correlate with two properties of the solute molecule: (a) total aliphatic and/or aromatic carbon number and (b) solute polarity as

TABLE V

COLUMN CHARACTERIZATION (ACETONITRILE-WATER)

Column	J_i	P_i	$r^\star$	$C_1^{\star\star}$	$C_2^{\star\star\star}$
ODS	+0.26	−0.55	0.71	0.072	0.093
C-8 330 m²/g (reference)	(0.00)	(0.00)	−	(0.000)	(0.000)
C-8 140 m²/g (standard)	−0.32	(0.00)	−	(0.000)	(0.000)
Phenyl	−0.54	1.24	0.75	−0.109	−0.014
TMS	−1.08	0.96	0.87	−0.082	−0.057
CN	−1.64	(1.00)	−	−0.055	−0.014
FD	−0.23	0.62	0.40	−0.109	−0.120

    * Correlation coefficient for plots of Fig. 8.
    ** Contribution of one methylene-group to $\Delta(\Delta t_g)_{xi}$.
    *** Contribution of one aromatic-carbon group to $\Delta(\Delta t_g)_{xi}$.
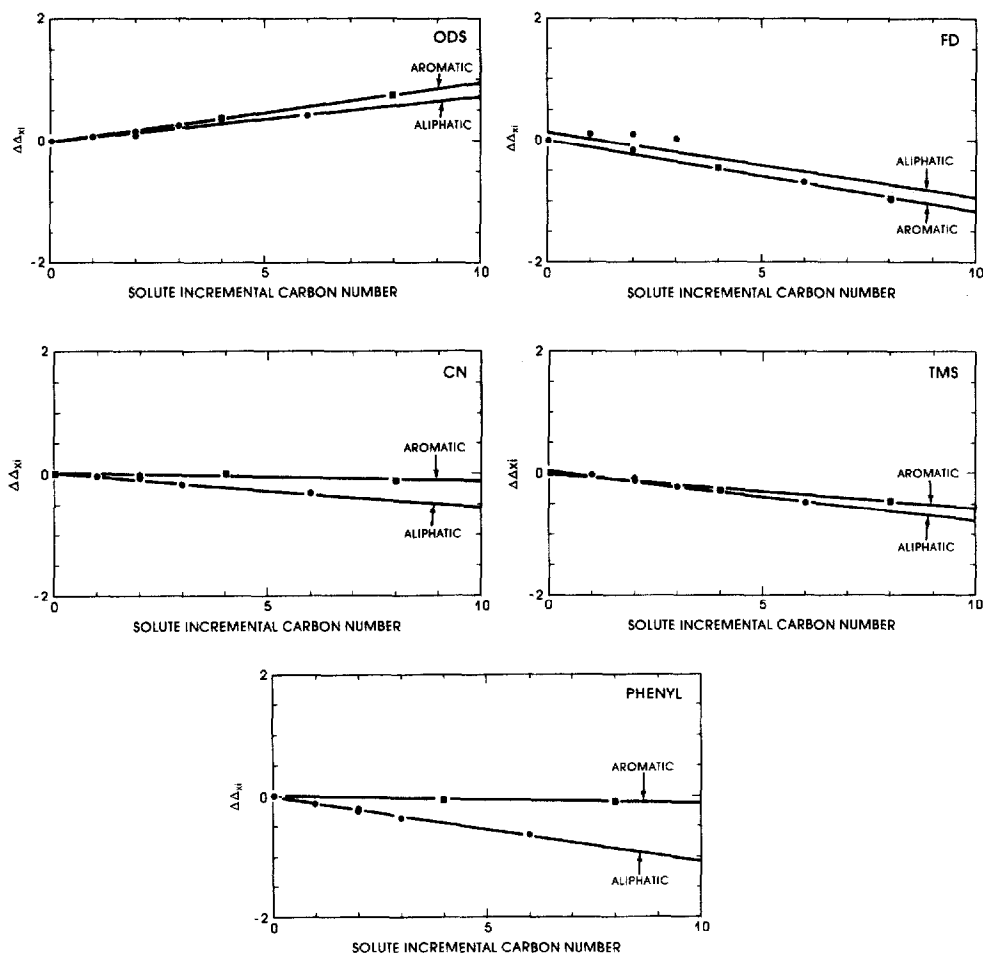
Fig. 7. Residual contributions to retention on different columns for addition of methylene (–CH$_2$–) or aromatic-carbon (–CH=) group to solute molecule. $\Delta\Delta_{xi}$ refers to value of $\Delta(\Delta t_g)_{xi}$ relative to lowest homologue or benzologue (methyl paraben, dimethyl phthalate and toluene).

measured by the number of polar functional groups in the solute molecule. Values of $\Delta(\Delta t_g)_{xi}$ also correlate with the column polarity P_i.

Relative values of $\Delta(\Delta t_g)_{xi}$, designated $\Delta\Delta_{xi}$ (see Appendix II) were plotted for each column and a series of homologues or benzologues vs. incremental solute carbon number; resulting plots are expected to be linear (eqn. 24). Fig. 7 shows these plots for alkyl parabens (n-alkyl esters of p-hydroxybenzoic acid) and di-n-alkyl phthalates as homologues, and toluene, 2-methylnaphthalene and 2-methylphenanthrene as benzologues. It is seen that the plots of Fig. 7 are generally linear, implying a constant contribution to the retention energy per carbon of the same type (cf. eqn. 22). From these plots for each column it is possible to derive a contribution to retention from either an aliphatic or aromatic carbon (C_1 and C_2 in eqn. 24). Values of these contributions are listed in Table V for each column and for both aliphatic and aromatic carbon. It is seen that larger solute carbon numbers favor increased values of $(\Delta t_g)_{xi}$
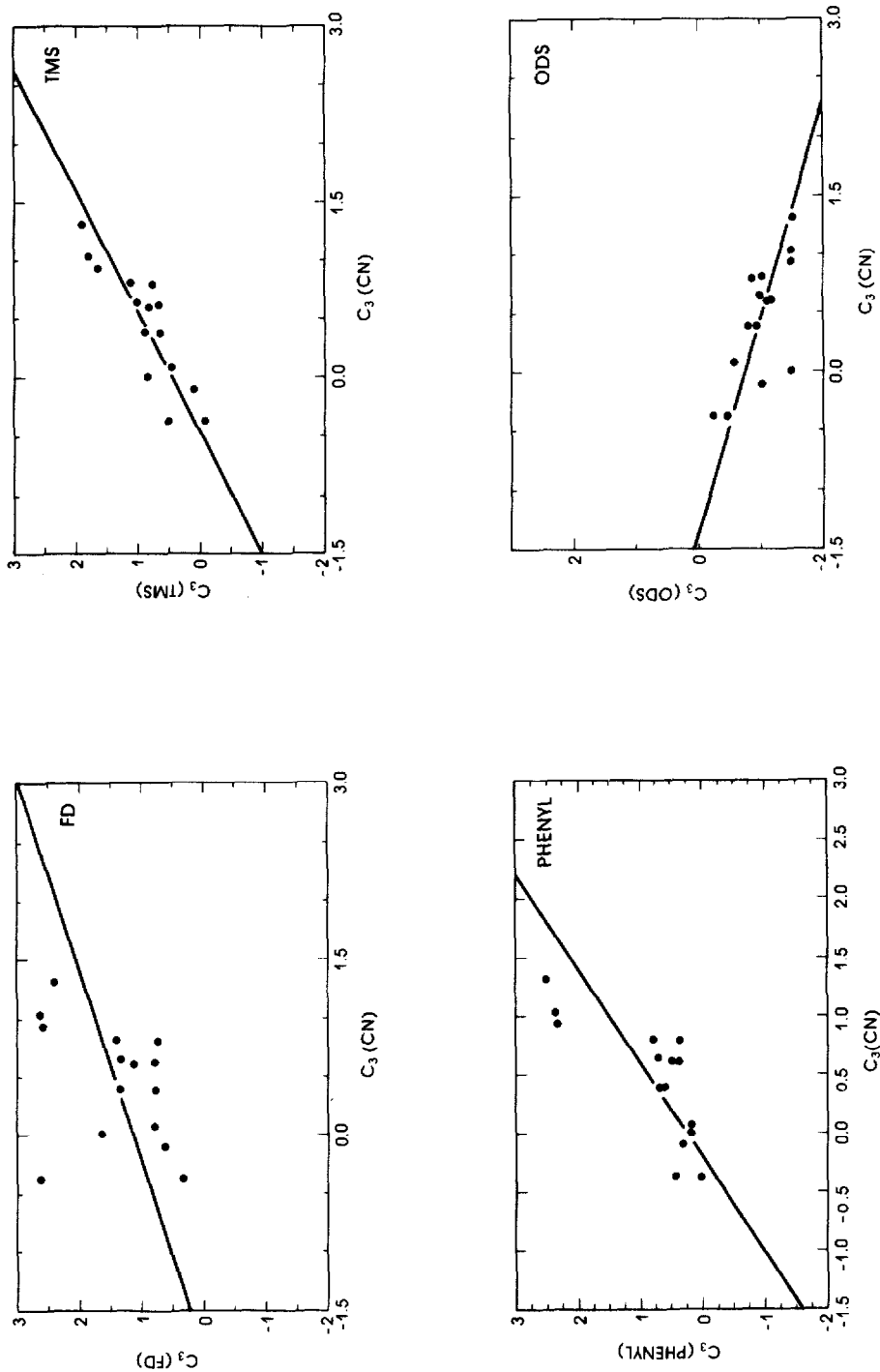
Fig. 8. Residual contribution to retention on different columns after correction for carbon number (values of C_3 from eqn. 24). Correlation of values for different columns with values for Zorbax CN. See Table V for correlation data.

TABLE VI

SUMMARY AND CORRELATION OF RETENTION DATA (METHANOL–WATER)

Column	$\overline{(\Delta t_a)_{xi}}$ (min)	$\overline{\Delta\varphi}$ vs. ODS (%)	Correlation data from Fig. 10			Standard deviations*
			m	a	r	
ODS	0.15	(0.0)	−0.79	−0.32	0.60	0.30 (0.24/0.18)
(r) C$_8$ 330 m^2/g	(0.00)	− 1	(0)	(0)	−	−
(s) C$_8$ 140 m^2/g	−0.60	− 5	(1.0)	(0)	−	−
Phenyl	−0.36	− 3	2.22	0.97	0.77	0.65 (0.41/0.50)
TMS	−1.74	−12	1.67	−0.73	0.71	0.53 (0.37/0.38)
CN	−5.48	−36	4.39	−2.83	0.88	1.12 (0.53/1.00)

* $X(Y/Z)$ format refers to: X = the total standard deviation for Δt_g values due to phase ratio/polarity and column–solute interactions; Y = the standard deviation around the best-fit lines of Fig. 4 due to column–solute interaction, and Z = the standard deviation due to phase ratio/polarity.
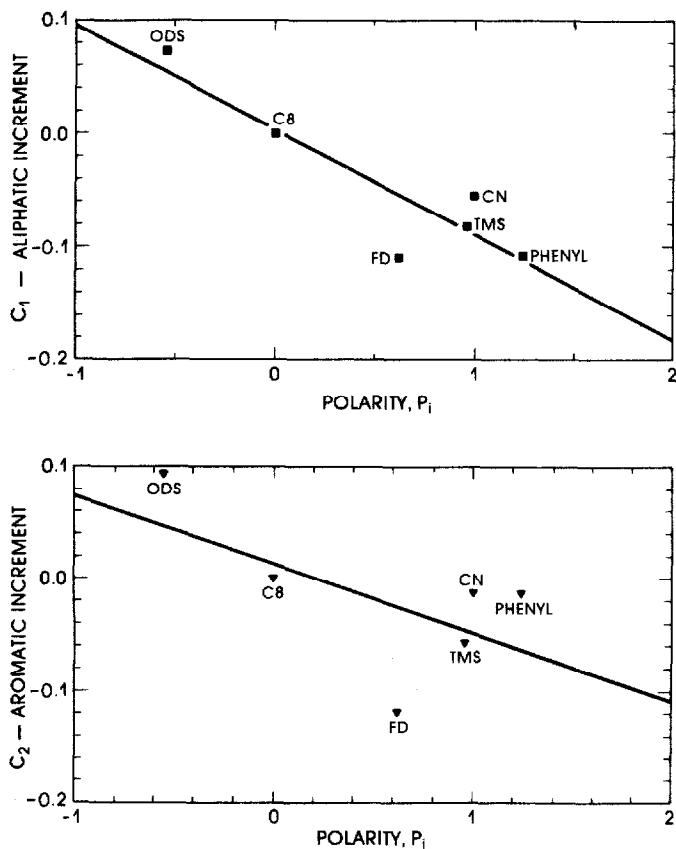

Fig. 9. Correlation of aromatic-carbon (C_2) and aliphatic-carbon (C_1) retention factors with column polarity.

on the ODS column (less polar) and decreased values on Phenyl, TMS and CN (more polar) columns.

Eqn. 24 can also be used to calculate values for C_3 for each compound and column; C_3 represents the net contribution to $\Delta(\Delta t_g)_{xi}$ (or solute–column interaction energy) after correction for the carbon number of the solute. It thus equals the net combined contribution to $\Delta(\Delta t_g)_{xi}$ of various substituent groups in the solute molecule. A plot of C_3 values for the cyano column vs. the number (n_p) of polar groups (Table III) in each solute molecule shows a rough correlation; $C_3 = 0.25 n_p - 0.01$, $r = 0.85$. The scatter is the result of (a) our use of total number of polar groups instead of recognizing the differences in polarity of individual groups; e.g., hydroxyl vs. carbonyl, (b) specific solute–column interactions other than those described by a single column polarity-parameter P, and (c) residual experimental error that is compounded by the subtraction of large values of t_g to arrive at final (small) values of C_3. If the polarity of the solute and column is largely responsible for values of $\Delta(\Delta t_g)_{xi}$, plots of C_3 for one column vs. values for a second column should be linear, as in eqn. 25. This is tested vs. the cyano column as x-axis in Fig. 8 for the remaining three columns (ODS, Phenyl and TMS) (y-axis). The slopes of these plots are proportional to the polarity of the column relative to cyano ($P_i = 1.00$ by definition for cyano). These slopes, P_i, are given in Table V for each column (see also eqns. 6 and 7). Also shown is the correlation coefficient r, which is reasonable for all but the fluorodecyl column (see below).

The correlation of C_1 values (incremental methylene retention) vs. column polarity P_i is tested in Fig. 9a. A close correlation is observed (except for the FD column), with greater retention of methylene groups on less polar columns as expected. Similar data for an aromatic-carbon group (C_2) are plotted vs. P_i in Fig. 9b, with poorer correlation. Specifically, the CN and Phenyl columns show stronger-than-expected retention of aromatic compounds, probably reflecting specific column–solute interactions not governed by simple column polarity. Preferential retention of aromatics vs. aliphatics on aromatic-base bonded phases has been reported by other workers (e.g., refs. 5 and 6).

The above evidence strongly supports column polarity as a significant parameter in accounting for remaining column-selectivity effects. The acquisition of more precise data for a larger solute base will no doubt qualify this generalization, and may demonstrate specific solute–column interactions that cannot be described by column polarity P_i alone. However, it is important to first determine what the forest looks like (the goal of this paper) before attempting to describe the individual trees in that forest.

Column selectivity with other organic solvents

Part of the preceding study was repeated with methanol in place of acetonitrile as the mobile phase solvent (t_g values in Appendix III). While these results were not analyzed in the same detail as for acetonitrile, our conclusion is that column selectivity is based on similar effects regardless of solvent. This is demonstrated by plotting $(\Delta t_g)_{xi}$ vs. $(\Delta t_g)_{xs}$ for methanol gradients in Fig. 10 (cf. similar plots in Fig. 3). Again linear plots are observed, and the various correlation data are summarized in Table VI. Comparisons of Tables IV and VI (acetonitrile vs. methanol) show only slightly poorer correlations with methanol than with acetonitrile. Again, values of m correlate
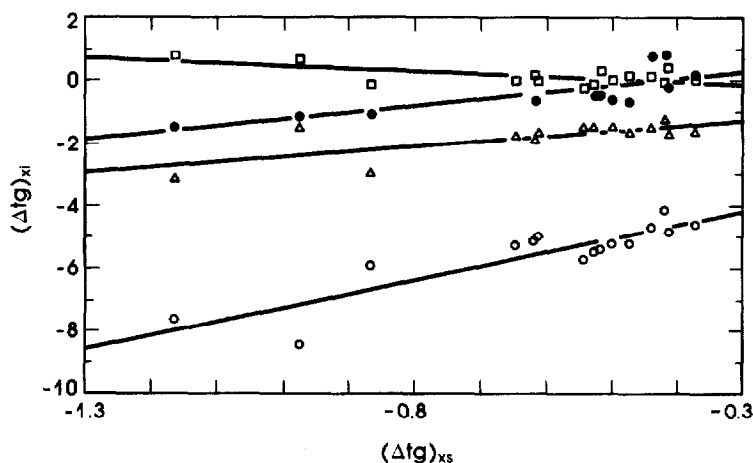
Fig. 10. Correlation of change in solute retention $\Delta(\Delta t_g)_{xi}$ for column i vs. $(\Delta t_g)_{xr}$ for column r (Zorbax C-8), according to eqn. 17. Methanol–water mobile phase. □, Zorbax ODS; ●, Phenyl; △, TMS; ○, CN.

with values of $(\Delta t_g)_{xi}$, as shown in Fig. 11 (cf. Fig. 5). Values of J_i for the various columns and methanol as solvent can be calculated, assuming that J_s is the same as in acetonitrile, -0.32. These J_i values are compared in Table VII. We see reasonable agreement between J_i values for both solvents, with the exception of TMS, whose phase ratio (J_i) is greater for methanol vs. acetonitrile as solvent. This may be the result of more effective shielding of surface silanol groups by methanol, thereby reducing the polarity of the trimethylsilyl phase and increasing its phase ratio/polarity term, J_i.

From eqn. 13, we see that $(\Delta t_g)_{xs}$ values for a given solute are proportional to corresponding S_x values. If we compare $(\Delta t_g)_{xs}$ values for acetonitrile or methanol as solvent we find a rough correlation (Fig. 12). This suggests that S_x values vary with solute structure in similar fashion regardless of the organic solvent used in the mobile phase (but note contradictory data of ref. 28).
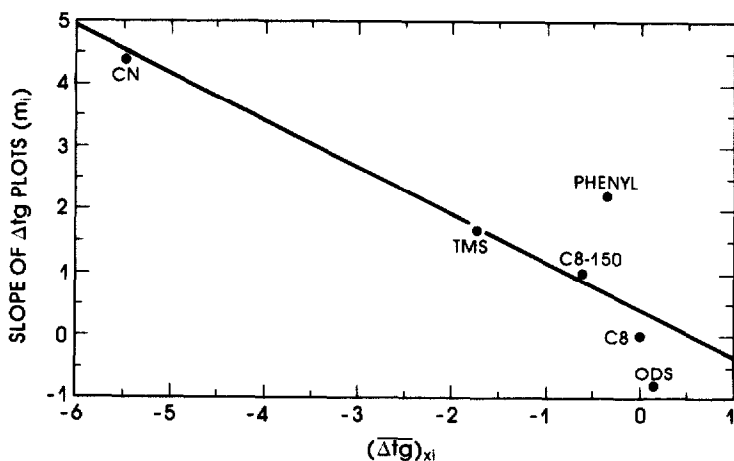

Fig. 11. Correlation of selectivity-slopes m_i from Fig. 10 with column strength $(\Delta t_g)_{xi}$, according to eqn. 31. $m_i = -0.75 \ (\Delta t_g)_{xi} + 0.41$; $r = 0.88$.

TABLE VII

J_i VALUES FOR ACETONITRILE AND METHANOL FOR THE VARIOUS COLUMNS

Column	J_i	
	Acetonitrile	Methanol
C_{18}	0.26	0.25
C_8 330 m²/g	0.00	0.00
C_8 140 m²/g	−0.32	(−0.32)
Phenyl	−0.54	−0.71
TMS	−1.08	−0.53
CN	−1.64	−1.40

Choosing columns of maximally different selectivity

Two column characteristics (the effective phase ratio J_i and the bonded-phase polarity P_i) appear to determine the main contributions of the column to separation selectivity. The relative importance of J_i and P_i can be assessed from the last column of Table IV. The last two numbers in each row (for each column) are the variation in t_g vs. the reference column due to (a) the polarity P_i (and other residual) effects and (b) the S_x/J_i effect. If we average these quantities for all columns (actually square root of squares) we obtain the net contribution to differences in t_g values among all columns (except fluorodecyl): S_j/J_i effect, ± 0.63 min (1 S.D.); P_i effect, ± 0.27 min. Thus the S_x/J_i effect is more than twice as important as the P_i effect as regards general column selectivity. Also, the P_i effect is slightly overstated, as it includes other contributions from specific solute/column interaction effects (which we have ignored here). The fluorodecyl column of Table IV is seen to have a larger P_i effect (± 0.62 min) vs. the S_x/J_i effect (± 0.14 min), but this is largely the result of specific column–solute interactions, as discussed in the following section.

Major change in column selectivity is thus associated with large differences in J_i values. On this basis, ODS ($J_i = 0.26$) and CN ($J_i = -1.64$) in Table V are seen to be maximally different (note similar J values for methanol as solvent). These two
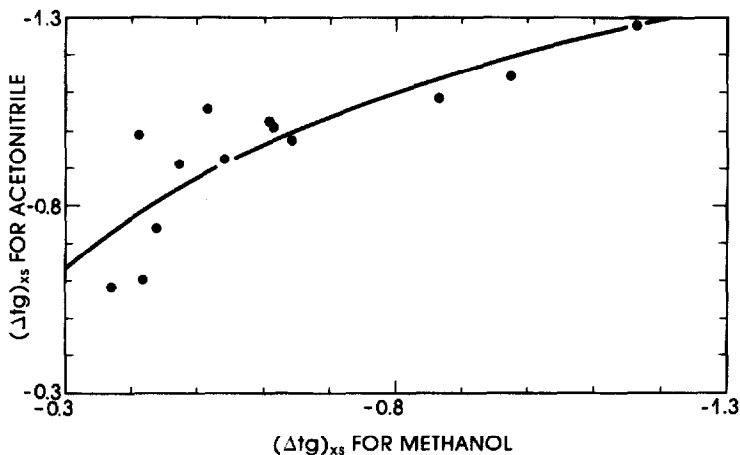
Fig. 12. Similarity of $(\Delta t_g)_{xs}$ values for acetonitrile vs. methanol as solvent.

columns are therefore logical choices of extremes in selectivity, and should be useful for this purpose in method development. The Phenyl column ($J_i = -0.54$) has an intermediate strength and the greatest polarity and should also prove useful as discussed in ref. 30. Further column-selectivity differences exist among all the columns of Table V, as shown by variation in values of P_i, C_1, and C_2. However, these effects will generally be much smaller than those determined by column J_i value (see ref. 30), although still useful for separating a given sample. The fluorodecyl column is an exception to this generalization, as discussed in the following section.

Fluorodecyl (FD) and other fluoro-substituted phases

The preceding discussion suggests that column selectivity in reversed-phase separations is governed by two primary effects: (a) differences in the effective phase ratio J_i among different columns, coupled with variation in S_x values for different solutes; (b) differences in the polarity of the stationary phase (bonded-phase plus silanols) P_i. This model provides a quantitative and self-consistent explanation of the various data collected, as summarized in Tables IV and V. However, these various correlations are notable poorer for the case of the FD column, vs. the remaining six columns of Table II, as summarized in Table VIII. Since the latter six columns are all based on a similar silica matrix (Zorbax of varying surface area), while the FD column is produced from a non-Zorbax silica, it is tempting to attribute differences in retention for the FD column to differences in the starting silica particles. However, we believe that this is not the case. Rather, it appears that these unaccounted-for selectivity effects on the FD column arise from the presence of a third contribution to selectivity that is associated mainly with the FD column. This third selectivity effect is the dispersive solubility parameter δ_d of the bonded phase[40], which will be much lower for a fluoroalkyl phase vs. the remaining phases of Table II.

Our reason for believing that the silica source is unimportant in explaining these anomalous solvophobic retention effects on the FD column is based on the study of Sadek and Carr[39]. These workers compared several fluoro-phase packings with an n-decyl packing. The FD and C_{10} packings used by them were produced by the same supplier, so it is probable that the same silica was used for these two packings (and in any case the silica for their C_{10} column is not Zorbax). Their results for the FD and C_{10} columns[36] are generally similar to retention data found by us for

TABLE VIII

ANOMALOUS CORRELATIONS FOR THE FD COLUMN

Correlation	Fig. or Table	Correlation index*	
		FD column	Other columns
J_i/S_x effect	Table IV, Fig. 4	$r = 0.22$	$r = 0.55-0.95$
m vs. $(\Delta t_R)_{xi}$	Fig. 6	$\Delta = -3.8$ in m	$\Delta = 0.0-0.4$
$C_{3\,(i)}$ vs. C_3 (CN)	Table V, Fig. 10	$r = 0.40$	$r = 0.71-0.87$
C_1 vs. P_i (methylene retention vs. column polarity)	Fig. 11a	$\Delta = -0.07$ for C_1	$\Delta = \pm 0.01-0.02$

* r is correlation coefficient; Δ is deviation from correlation (least squares) line.

FD and Zorbax C-8 columns. So it appears that the silica source is not a major factor in the anomalous hydrophobic retention on the FD column. Likewise, the data of Sadek and Carr[39] generally parallel findings by other workers[10,11] who compared retention on FD vs. C_{10} or C_{18}.

First consider the evidence that the FD column is relatively polar, as found by us ($P_i = 0.62$, Table V). Sadek and Carr (in agreement with refs. 10 and 11) find generally stronger retention of more polar, nonionizable groups (NO_2, $-COCH_3$, $-CHO$ and $-CN$) vs. C_{10}, and weaker retention of less polar groups (phenyl, $-CH_3$, $-CH_2$, etc.). FD is also a weaker column ($J_i = -0.23$), which is consistent with its greater polarity. The greater polarity of the FD column is surprising in one respect: previous workers[10,39] have noted that the lower solubility parameters and decreased polarity of fluoroalkyl groups should lead to decreased polarity of this phase. Apparently other factors play a dominant role; e.g., configuration of the FD chains, relative adsorption of organic solvent molecules, silanol accessibility, etc. At this point there is not enough data to draw any conclusion as to the cause of the greater polarity of the FD column as compared to C_8 or C_{10}.

Returning to the anomalous retention of FD vs. other reversed-phase columns (Table VIII), the much lower dispersion solubility parameter of this phase provides a likely explanation of these effects. In most HPLC systems, dispersion contributions to retention are of minor importance, because the dispersion interactions between solute molecules and either the mobile phase or the stationary phase are similar in magnitude. This is the result of similar dispersion solubility parameters δ_d for various chromatographic phases[40]; i.e., the dispersion interaction energy between a solute molecule and the surrounding phase will be proportional to the δ_d values of solute and the surrounding phase.

The importance of these δ_d effects can be seen most clearly in the case of halogen-substituted compounds as solutes. A halogen substituent-group in either an alkane or aromatic molecule has a dipole moment that does not vary significantly among $-F$, $-Cl$, $-Br$ or $-I$ groups. The hydrogen bonding tendency of a halogen group is also insignificant. This means that the polarity of different halogen groups is essentially constant, and the relative retention of these groups will be governed largely by their differing dispersion solubility parameters. If we compare the refractive indices of the mono-halogen-substituted benzenes (e.g., ref. 39), we find that refractive index and δ_d (see ref. 40) increase in the sequence $-F < -Cl < -Br < -I$. The energy of interaction of these groups with a reversed-phase packing will be proportional to the product of their individual solubility parameters and the solubility parameter of

TABLE IX

RETENTION OF MONOHALOGEN-SUBSTITUTED BENZENES ON A C_{10} AND FD COLUMN

Solute	Log k' vs. benzene	
	C_{10}	FD
Fluorobenzene	+0.01	+0.09
Chlorobenzene	+0.26	+0.14
Bromobenzene	+0.33	+0.12
Iodobenzene	+0.45	+0.11

the packing. The δ_d value of a C_8 or C_{10} column will be much larger than for a FD column, so there will be a larger increase in retention for the series –F:–Cl:–Br:–I on a C_{10} column vs. the FD column. This is confirmed by Sadek and Carr (Table IX). The absolute values of these group retention factors can be explained in terms of the δ_d value of the mobile phase (≈ 6.2 for methanol–acetonitrile–water mixtures) vs. a lower δ_d value for FD and the higher δ_d value for C_{10}, as well as by the greater retention of larger solute molecules in reversed-phase systems (normal solvophobic effect; cf. ref. 22)*.

The above discussion provides an answer to why the FD phase preferentially retains fluoro-substituted solutes vs. C_8 or C_{10}: the δ_d values are better matched in the case of the FD column ("like prefers like", see ref. 41). The above example for the halogen-substituted benzenes also suggests that these dispersion interactions can explain the anomalous retention effects on the FD column (Table VI). Although dispersion contributions tend to cancel for other reversed-phase bonded phases, this will be less likely for a phase of quite different δ_d value; solubility parameter theory predicts that these effects (related to small differences in δ_d for various solute molecules) will be magnified for phases with very different values of δ_d; i.e., the dispersion interaction energy is proportional to $[(\delta_d)_1 - (\delta_d)_2]^2$ for two interacting molecules or species, 1 and 2.

Reversed-phase separation on silica

Horváth et al.[42] have noted that mobile phases rich in water yield solvophobic separation on bare silica packings; i.e., essentially reversed-phase behavior. Limited data were collected for standard gradient runs (15 min, acetonitrile–water) and several of the standard solutes of Table III. A value of $\overline{(\Delta t_g)_{xi}}$ equal to -7.9 min was determined from these data, confirming that silica is an extremely weak reversed-phase packing; cf. values of $\overline{(\Delta t_g)_{xi}}$ for other columns of Table IV (we estimate $\Delta \varphi$ vs. ODS column at -50% (v/v) acetonitrile for silica).

CONCLUSIONS

Column selectivity in reversed-phase HPLC has been studied as a function of solute structure and column type. The resulting data allow certain conclusions regarding "solvophobic" selectivity, in the absence of "chemical" selectivity based on hydrogen bonding, ion exchange and/or chemical complexation between sample and column packing. Our results should be useful for HPLC systems where these latter chemical effects have been minimized, as by the selection of a suitable pH or use of appropriate additives for the mobile phase (e.g., alkylamines).

Changes in solvophobic selectivity can be correlated in terms of the following effects:

(a) Reversed-phase columns differ in "strength" or their effective phase ratio (J value) as a result of differences in silica surface area, alkyl chain length (and surface coverage), and the polarity of the bonded phase (which includes surface silanols); differences in J values lead to corresponding shifts in retention for all solutes on a given column (same mobile phase), but no change in band spacing as long as the same mobile phase is used.

---

* Molecular size increases in the sequence: fluorobenzene < chlorobenzene < bromobenzene, etc.

(b) For columns differing in J values, the strength of the mobile phase must be adjusted (by varying water content) to maintain sample retention in an optimum k' range (*e.g.*, $1 \leqslant k' \leqslant 10$). The S values (equal $-d[\log k']/d\varphi$) of two compounds can differ; this in combination with the change in mobile-phase composition will then result in significant changes in band spacing. This is the major contribution to column selectivity that we have observed.

(c) While the column strength or J value includes contributions from stationary phase polarity (as measured for average solutes), individual solutes vary in polarity, leading to a further contribution of column polarity to selectivity; *i.e.*, more polar solute molecules are preferentially held on more polar columns. Column polarity can be measured by a parameter P, which further characterizes column selectivity. However, this contribution to selectivity is less important, and furthermore tends to parallel change in column J values.

(d) Fluoroalkyl columns exhibit additional selectivity effects due to the lower dispersion-solubility parameter δ_d of these phases. This leads to differences in retention *vs.* other columns which are generally less important; *e.g.*, preferential retention of fluoro-substituted solutes.

The practical consequences of our findings are summarized in ref. 30. It appears that solvophobic contributions to column selectivity are less complex than had originally been believed. Maximum differences in column selectivity are predicted for columns with maximum differences in effective phase ratio and polarity. The data of Table V suggest Zorbax ODS, CN and Phenyl as good choices for varying J, P and the ratio J/P over wide limits. A similar 3-column set (C_8, phenyl, cyanopropyl) has in fact been shown[43] to afford different selectivities for the PTH amino acids as solutes. While our data are based mainly on Zorbax packings, we feel that these conclusions should also apply to fully-bonded reversed-phase packings from other suppliers.

SYMBOLS

a	The intercept of the best-fit line for plots of $(\Delta t_g)_{xi}$ for column i *vs.* $(\Delta t_g)_{xs}$ for the standard column s (a lower-surface-area C_8) (eqn. 17)
b	The gradient steepness parameter, equal to $(S\Delta\varphi/t_G)$ (eqn. 3)
C_1	A constant reflecting the incremental contribution of an aliphatic carbon to $\Delta(\Delta t_g)_{xi}$ (eqn. 23)
C_2	A constant reflecting the incremental contribution of an aromatic carbon to $\Delta(\Delta t_g)_{xi}$ (eqn. 24)
C_3	The value of $\Delta(\Delta t_g)_{xi}$ after subtracting contributions from aromatic and aliphatic carbons (eqns. 23 and 24)
C_4, C_5	Constants for relating $\Delta(\Delta t_g)_{xi}$ values on two columns (eqn. 25)
i, j	As subscripts, designations for different test columns
J'_i	The combined phase ratio/polarity term for column i ("effective phase ratio") (eqn. 7)
J_i	The "effective phase ratio" of column i relative to that of the reference column r, (Zorbax C-8, see Table II) (eqn. 11)
k_{xi}	The k' value $(t_R-t_0)/t_0$ for compound X on column i in an isocratic experiment (eqns. 5 and 6)
k_0	The k' value which would be obtained in an isocratic experiment using the initial mobile phase composition of a gradient (eqn. 2)

$\bar{k}$ The average k' value in gradient elution (eqn. 1).

K^0_{xi} The distribution constant for solute X and stationary phase i (eqn. 5), with φ equal to value at start of gradient

K_{xi} The (approximately) polarity-corrected contribution to K^0_{xi} (eqn. 6)

K_{xi}/K_{xr} The solute-column interaction parameter representing residual selectivity effects independent of J and S (eqn. 10 for φ equal to value at start of gradient)

LSS   Linear solvent strength (see refs. 31–33)

m_i Equal to J_i/J_s, the slope of a plot of $(\Delta t_g)_{xi}$ vs. $(\Delta t_g)_{xs}$, where r is the reference column (Zorbax C-8, s is the standard column (Zorbax 150-C8 and i is a test column (eqn. 18)

P_i A relative column-polarity parameter, equal to the slope of a plot of C_3 for a test column i versus C_3 for the CN column (Fig. 8)

R_M Log k'

r   Subscript referring to the reference column; for this paper, Zorbax C-8 (330 m^2/g)

s   Subscript referring to the standard column, a Zorbax 150-C8 (140 m^2/g)

S The negative of the slope of a plot of log k versus volume fraction φ of organic solvent in the mobile phase; equal $-d(\log k')/d\varphi$. In this paper, S for a given solute is assumed to be independent of the stationary phase (column) used

S_x The S value for a specific compound X

$\bar{S}$ The average of the S_x values for a given set of test-solutes

t_D The time between a programmed change in solvent composition and the actual time that composition change reaches the head of the column (min)

t_0 Column dead time (min)

t_g The retention time obtained for a solute in a gradient separation (eqn. 2) (min)

$(t_g)_{xi}$ Value of t_g for solute X and column i

t_G Gradient time; the time during the gradient during which φ changes (min)

t_R The isocratic retention time of a solute (min)

x   Subscript denoting the solute used: e.g., $(t_g)_x$ is the gradient retention time for compound X

$\Delta\Delta_i$ In homologue runs, $\Delta(\Delta t_g)_{xi}$ values minus $\Delta(\Delta t_g)_{xi}$ for a reference compound (methyl paraben, dimethyl phthalate, toluene, respectively) (Fig. 7)

$(\Delta t_g)_{xi}$ The t_g value for solute X on column i minus t_g for solute X on reference column r, equal to $[(t_g)_{xi} - (t_g)_{xr}]$ (eqn. 9)

$\Delta(\Delta t_g)_{xi}$ From a plot of $(\Delta t_g)_{xi}$ vs. $(\Delta t_g)_{xs}$, the difference between the actual value of $(\Delta t_g)_{xi}$ and that predicted by the best-fit line (eqn. 20)

$\Delta\varphi$ The change in volume-fraction φ of the strong solvent in the mobile phase during a gradient (eqn. 2); also the change in φ vs. Zorbax ODS required to maintain constant k' values for a sample (Table IV)

φ The volume fraction of strong solvent in the mobile phase

ψ_i The phase ratio for a column packing i

δ_d The dispersion solubility parameter (ref. 41)

APPENDIX I

Retention data for standard gradient (min) acetonitrile–water system

	ODS	C-8	150-C8	Phenyl	CN	TMS	FD	C-8 (30 m)
Set No. 1								
Benzyl alcohol	7.05	7.24	6.15	6.48	3.54	4.62	4.39	8.76
Benzyl methyl amine	9.18	9.04	7.90	8.38	5.51	6.70	6.20	11.75
Butyl paraben	11.48	11.61	10.70	10.71	9.32	9.99	8.96	17.35
Chlorpropham	12.80	12.68	11.67	11.76	10.10	10.73	9.68	19.24
Corticosterone	10.07	10.15	9.41	10.07	8.63	9.21	7.86	14.79
Cortisone	8.93	9.11	8.51	9.12	8.03	8.54	7.16	12.98
Dexamethasone	9.61	9.73	9.15	9.64	8.60	9.00	7.63	14.16
Dibutylphthalate	15.38	14.87	13.81	13.55	11.32	12.40	11.78	23.58
Diethylphthalate	11.96	11.85	10.83	11.13	9.12	10.05	9.29	17.56
Fluorobenzene	11.40	11.05	9.77	9.92	6.60	8.22	8.33	15.48
Hexafluorobenzene	12.95	12.62	11.48	11.58	8.42	10.30	11.83	18.86
Methyl paraben	8.08	8.47	7.55	8.05	6.29	6.90	5.80	11.26
o-Nitrophenol	9.96	9.51	8.50	9.10	6.00	7.05	6.53	13.10
Propachlor	11.42	11.38	10.41	10.78	8.79	9.74	8.90	16.65
Tri-*p*-tolyl phosphate	15.91	15.39	14.40	14.28	12.03	13.01	11.97	24.86
Ethyl paraben		9.62		9.06	7.72			13.45
Propyl paraben		10.68		9.98	8.53			15.51
Set No. 2								
Benzyl alcohol	6.81	7.18	6.35	6.58	3.92	4.65	4.15	
Toluene	12.44	12.04	10.94	10.86	8.47	9.22	8.72	
1-Methylnaphthalene	14.25	13.58	12.60	12.51	10.63	10.89	9.88	
1-Methylphenanthrene	15.76	14.72	13.74	13.63	11.66	11.86	10.52	
Dimethylphthalate	9.62	9.94	9.16	9.57	7.63	8.40	7.47	
Diethylphthalate	11.61	11.79	10.96	11.15	9.20	9.97	9.13	
Dibutylphthalate	15.98	14.85	13.92	13.59	11.41	12.29	11.58	
Dioctylphthalate	19.20	18.27	17.28	16.12	13.27	14.89	14.34	
Methyl paraben	7.88	8.54	7.69	8.12	6.58	6.86	5.59	
Ethyl paraben	9.12	9.70	8.86	9.14	7.72	8.02	6.87	
Propyl paraben	10.29	10.78	9.92	10.09	8.70	8.98	7.73	
Butyl paraben	11.34	11.73	10.86	10.90	9.48	9.76	8.80	

Retention data for the second data set (the homologue study) were obtained using the same columns six months after the initial set was completed. Agreement between the two data sets is two- to threefold poorer than the day-to-day precision in either set. The second set was used only for determination of the aliphatic and aromatic increment values.

APPENDIX II

Illustrative calculations for the Zorbax CN column (i)

(1) Δt_g

Compound name	$(t_g)_{xr}$*	$(t_g)_{xs}$*	$(t_g)_{xi}$*	$(t_g)_{xs} - (t_g)_{xr}$ $= (\Delta t_g)_{xs}$	$(t_g)_{xi} - (t_g)_{xr}$ $= (\Delta t_g)_{xi}$
Dexamethasone (D)	9.73	9.15	8.60	−0.58	−1.13
Fluorobenzene (FB)	11.05	9.77	6.60	−1.28	−4.45

(2) $\Delta\Delta t_g$

From plot of $Y = (\Delta t_g)_{xi}$ *versus* $X = (\Delta t_g)_{xs}$ using all 15 original test compound a best fit line is calculated with the slope, m, equal to 5.14 and intercept, a, equal to 2.13.

Compound	$(\Delta t_g)_{xs}$	Predicted $(\Delta t_g)_{xi} - m (\Delta t_g)_{xs} + a$	$(\Delta t_g)_{xi}$	$\Delta(\Delta t_g)_{xi}$
D	−0.58	−0.85	−1.13	−0.28
FB	−1.28	−4.45	−4.45	0

(3) Carbon increment calculation

Compounds (X)	No. of carbons		$\Delta(\Delta t_g)_{xi}$	$\Delta\Delta_i$
	Aromatic	Incremental		
Toluene	6	0	−0.027	0.0
1-Methylnaphthalene	10	4	−0.030	−0.003
1-Methylphenanthrene	14	8	−0.141	−0.114

(4) Corrected $\Delta\Delta t_g$

From the plot of the homologous series the aliphatic increment, C_1, is −0.055 and the aromatic increment, C_2, is −0.014.

Compound	No. of C (aliphatic)	No. of C (aromatic)	Correction	$\Delta(\Delta t_g)_{xi}$	C_3
D	22	0	−1.210	−0.28	−1.49
FB	0	6	−0.084	0	−0.08

* In this paper r, the reference column, is a 330 m²/g Zorbax C-8; s is a 140 m²/g Zorbax C-8 and for this example *i* is a Zorbax CN.

APPENDIX III

Retention data for standard gradient (min) methanol–water system

	ODS	C₈	150-C₈	Phenyl	TMS	CN
Benzyl alcohol	8.35	8.44	7.57	7.37	5.53	2.53
Butyl paraben	13.80	13.65	13.18	12.96	12.06	8.45
Chlorpropham	14.22	14.06	13.44	13.41	12.23	8.97
Corticosterone	13.15	13.02	12.58	13.80	11.55	8.38
Cortisone	11.74	11.79	11.37	12.61	10.59	7.68
Dexamethasone	12.84	12.74	12.37	12.98	11.15	8.19
Dibutylphthalate	16.38	16.05	15.54	15.58	14.24	10.68
Diethylphthalate	13.27	13.26	12.65	13.11	11.68	8.28
Ethyl paraben	11.26	11.39	10.86	10.93	9.99	5.94
Fluorobenzene	12.80	12.01	10.84	10.51	8.94	4.42
Hexafluorobenxene	14.82	14.07	13.09	12.93	12.66	5.66
Methyl paraben	9.69	9.91	9.37	9.60	8.49	4.22
Propachlor	13.14	13.14	12.50	13.09	11.45	7.91
Propyl paraben	12.65	12.63	12.13	12.04	11.14	7.4
Tri-*p*-tolyl phosphate	17.13	16.74	16.33	16.56	15.08	11.94

REFERENCES

1 L. C. Sander and S. A. Wise, *Anal. Chem.*, 56 (1984) 504.
2 H. Engelhardt, B. Dryer and H. Schmit, *Chromatographia*, 16 (1982) 11.
3 J. K. Rozylo and I. Malinowska, in H. Kalasz (Editor), *New Approaches in Liquid Chromatography*, Elsevier, Amsterdam, 1984, p. 85.
4 M. Verzele and C. Dewaele, *Chromatographia*, 18 (1984) 84.
5 N. Tanaka, K. Sakagami and M. Araki, *J. Chromatogr.*, 199 (1980) 327.
6 N. Tanaka, Y. Tokuda, K. Iwaguchi and M. Araki, *J. Chromatogr.*, 239 (1983) 761.
7 R. M. Smith, *J. Chromatogr.*, 237 (1982) 144.
8 H. Engelhardt and G. Ahr, *Chromatographia*, 14 (1981) 227.
9 W. Melander, J. Stoveken and Cs. Horváth, *J. Chromatogr.*, 199 (1980) 35.
10 G. E. Berendsen, K. A. Pikaart and L. de Galan, *Anal. Chem.*, 52 (1980) 1990.
11 H. A. H. Billiet, P. J. Schoenmakers and L. de Galan, *J. Chromatogr.*, 218 (1981) 443.
12 S. A. Wise, L. C. Sander and W. E. May, *J. Liquid Chromatogr.*, 6 (1983) 2709.
13 S. A. Wise and W. E. May, *Anal. Chem.*, 55 (1983) 1479.
14 G. E. Berendsen, K. A. Pikaart and L. de Galan, *J. Liquid Chromatogr.*, 10 (1980) 1437.
15 L. Trojer and L. Hansson, *J. Chromatogr.*, 262 (1983) 183.
16 T. Daldrup and B. Kardel, *Chromatographia*, 18 (1984) 81.
17 I. D. Wilson, C. R. Bielby and E. D. Morgan, Jr., *J. Chromatogr.*, 238 (1982) 97.
18 A. P. Goldberg, *Anal. Chem.*, 54 (1982) 342.
19 R. M. Smith, *J. Chromatogr.*, 236 (1982) 321.
20 R. M. Smith, *Anal. Chem.*, 56 (1984) 256.
21 J. J. DeStefano, A. P. Goldberg, J. P. Larmann and N. A. Parris, *Ind. Res. Dev.*, 4 (1980) 99.
22 W. R. Melander and Cs. Horváth, in Cs. Horváth (Editor), *High-performance Liquid Chromatography*, Vol. 2, Academic Press, New York, 1980, p. 113.
23 K. E. Bij, Cs. Horváth, W. R. Melander and A. Nahum, *J. Chromatogr.*, 203 (1981) 65.
24 E. Papp and G. Vigh, *J. Chromatogr.*, 282 (1983) 59.
25 E. Papp and G. Vigh, *J. Chromatogr.*, 259 (1983) 49.
26 A. Tchapla, H. Colin and G. Guiochon, *Anal. Chem.*, 56 (1984) 621.
27 T. L. Hafkenscheid and E. Tomlinson, *J. Chromatogr.*, 264 (1983) 47.
28 P. J. Schoenmakers, H. A. H. Billiet and L. de Galan, *J. Chromatogr.*, 185 (1979) 179.
29 P. J. Schoenmakers, H. A. H. Billiet and L. de Galan, *Chromatographia*, 15 (1982) 205.

30 P. E. Antle and L. R. Snyder, *LC Magazine*, 2 (1984) 840.
31 L. R. Snyder, in Cs. Horváth (Editor), *High-performance Liquid Chromatography*, Vol. 1, Academic Press, New York, 1980, p. 207.
32 M. A. Quarry, R. L. Grob and L. R. Snyder, *J. Chromatogr.*, 285 (1984) 1.
33 M. A. Quarry, R. L. Grob and L. R. Snyder, *J. Chromatogr.*, 285 (1984) 19.
34 K. Karch, I. Sebestian and I. Halász, *J. Chromatogr.*, 122 (1976) 3.
35 H. E. Gerke, F. Eisenbeiss and K.-F. Krebs, in L. Peichang and E. Bever (Editors), *Proc. Sino-West German Symp. on Chromatogr.*, Science Press, Beijing, 1983, p. 416 (Fig. 16).
36 B. Pekić, S. M. Petrocić and B. Slavica, *J. Chromatogr.*, 268 (1983) 237.
37 L. R. Snyder and J. J. Kirkland, *Introduction to Modern Liquid Chromatography*, Wiley Interscience, New York, 2nd ed., 1979, p. 580.
38 F. M. Rabel and E. T. Butts, *LC Magazine*, 1 (1983) 42.
39 P. C. Sadek and P. W. Carr, *J. Chromatogr.*, 288 (1984) 25.
40 B. L. Karger, L. R. Snyder and C. Eon, *Anal. Chem.*, 50 (1978) 2126.
41 L. R. Snyder, *ChemTech*, 9 (1979) 750.
42 A. Nahum and Cs. Horváth, *J. Chromatogr.*, 203 (1981) 53.
43 J. L. Glajch and J. J. Kirkland, *Anal. Chem.*, 55 (1983) 319A.